Nuclear Instruments and Methods in Physics Research B 378 (2016) 31–37

Contents lists available at ScienceDirect

Nuclear Instruments and Methods in Physics Research B

journal homepage: www.elsevier.com/locate/nimb

Molecular dynamics study of radiation damage and microstructure evolution of zigzag single-walled carbon nanotubes under carbon ion incidence

Huan Li [a], Xiaobin Tang [a,b,*], Feida Chen [a], Hai Huang [a], Jian Liu [a], Da Chen [a,b]

[a] Department of Nuclear Science & Engineering, Nanjing University of Aeronautics and Astronautics, Nanjing, China
[b] Jiangsu Key Laboratory of Nuclear Energy Equipment Materials Engineering, Nanjing, China

ARTICLE INFO

Article history:
Received 29 January 2016
Received in revised form 21 March 2016
Accepted 22 April 2016

Keywords:
Single-walled carbon nanotubes
Radiation damage
Microstructure evolution
Molecular dynamics

ABSTRACT

The radiation damage and microstructure evolution of different zigzag single-walled carbon nanotubes (SWCNTs) were investigated under incident carbon ion by molecular dynamics (MD) simulations. The radiation damage of SWCNTs under incident carbon ion with energy ranging from 25 eV to 1 keV at 300 K showed many differences at different incident sites, and the defect production increased to the maximum value with the increase in incident ion energy, and slightly decreased but stayed fairly stable within the majority of the energy range. The maximum damage of SWCNTs appeared when the incident ion energy reached 200 eV and the level of damage was directly proportional to incident ion fluence. The radiation damage was also studied at 100 K and 700 K and the defect production decreased distinctly with rising temperature because radiation-induced defects would anneal and recombine by saturating dangling bonds and reconstructing carbon network at the higher temperature. Furthermore, the stability of a large-diameter tube surpassed that of a thin one under the same radiation environments.

1. Introduction

Single-walled carbon nanotubes (SWCNTs), as an emerging quasi-one-dimensional material with extraordinary mechanical and electrical properties, have extensive applications such as sensors, thin-film transistors [1,2], and high-performance composites [3]. Carbon nanotube-based tape offered an excellent synthetic option as a dry conductive reversible adhesive in microelectronics, robotics and aerospace application [4], and carbon nanotube matrices combined with quantum dot might be used in space photovoltaic devices [5]. These CNTs-based aerospace devices may be exposed to harsh radiation environments, and they are continuously bombarded by energetic particles under these severe conditions. Unfortunately, the radiation-induced structural changes in CNTs significantly affect their physical, electrical and morphological properties [6–10]. Furthermore, the structure and properties of CNTs can be tailored and modified with various forms of ionizing radiation, including high-energy gamma rays, electrons and ions [11]. Vacancies and interstitials created by displacement cascades under abundant high-energy charged particles in SWCNTs would eventually form defect clusters (voids, interstitial clusters and non-hexagonal rings) due to the accumulation effects.

Previous works on the ion beam interacting with CNTs focused on cutting and doping CNTs. For example, energetic focused Ga^+ ions beam was applied to thin, slice, wield and change the structure and composition of CNTs at precise positions along the nanotube axis [12]. However, the microstructure evolution of defects generated in carbon nanotubes under focused ion irradiation was difficult to obtain from experiments. In the meantime, the prediction of structural configuration was allowed through computational and theoretical simulations after exposure to an energetic particle beam. M. Khazaei et al. adopted *ab initio* molecular dynamics simulations to clarify Cs^+ insertion and adsorption processes which is shot toward the cap and stem of two kinds of armchair nanotubes by considering the impact angle, impact position and the kinetic energy of dopant [13]. T. Kato et al. illustrated the damage-free and position-selective encapsulation of Cs into SWCNTs, and the minimum energy threshold of Cs-ion doping matched well with the value obtained by *ab initio* simulation [14]. Molecular dynamics (MD) simulation was employed to study the improved inter-tube coupling [15], and the structural and formation yields of atomic-scale defects [16] in SWCNTs bundles through C and Ar ion irradiation by O'Brien and E. Salonen, respectively. S. K. Pregler et al. also used MD simulation to investigate the

* Corresponding author at: Department of Nuclear Science & Engineering, Nanjing University of Aeronautics and Astronautics, Nanjing, China.
E-mail address: tangxiaobin@nuaa.edu.cn (X. Tang).

http://dx.doi.org/10.1016/j.nimb.2016.04.043
0168-583X/

surface structure and mechanical properties of polystyrene-carbon nanotube composites under Ar ion irradiation [17]. Furthermore, the stability of armchair SWCNTs with a small tube diameter under ion irradiation with the energy range of 25 eV–1 keV was investigated by Z. Xu in detail [18]. E.C. Neyts et al. indicated that ion bombardment in the lower energy window of 10–25 eV actually allowed radiation-induced defects to be healed resulting in an enhanced nucleation of the carbon nanotube cap through combining experiment and MD simulation [19,20].

However, it should be noted that the tube diameter, chirality, temperature and incident ion fluences are the critical influencing factors of the radiation damage and microstructure evolution of carbon nanotubes, and that detailed local damage information at different sites of SWCNTs could not be determined explicitly because the impact positions are randomly selected within the minimum irreducible area in the primitive cell of carbon nanotubes. Therefore, it is necessary to explore more details of the above critical factors.

In the present work, molecular dynamics simulations were used to explore the radiation damage and microstructure evolution of SWCNTs under various irradiation conditions. Incident carbon ion was chosen since it introduced no impurity into the system and enabled efficient momentum transfer due to the match between the mass of the impinging ion and target atoms. We classified the incident sites of SWCNTs into three types to investigate the defect production mechanism and evolution of zigzag carbon nanotubes under ion irradiation. We studied the influence of ion irradiation on different sites of SWCNTs under the incident ion fluences ranging from 2×10^{13} ions/cm^2 to 2×10^{14} ions/cm^2. The incident ion fluence range was comparable to that in the aerospace environment [21]. As a critical factor that affected the evolution of radiation-induced defects, the influence of temperature on SWCNTs was investigated as well. Moreover, the role of the tube diameter was also discussed in the stability of SWCNTs under irradiation.

2. Simulation methods

The public-domain parallelized program LAMMPS code [22] distributed by Sandia National Laboratories was used to perform all simulations in the study. The interactions between carbon atoms in SWCNTs were described by the adaptive intermolecular reactive empirical bond order (AIREBO) potential [23], which was appropriate to study the reactivity in molecular condensed-phase hydrocarbon systems. Tersoff-like [24] potential, which was smoothly connected with the Ziegler–Biersack–Littmark (ZBL) universal repulsive potential [25] at short interatomic distances using a Fermi function, was employed to simulate realistically close collisions between incident and target atoms. This type of potential has been successfully applied to simulate the irradiation and implantation of carbon nanomaterials [26,27]. The high-end cutoff radius was optimized to the value 2.46 Å and the Tersoff potential parameter λ_3 was set equal to λ_2 as in Ref. [27]. As the incident ion energies were low and the nuclear stopping governed the collisional phase, electronic stopping was not taken into consideration.

The chiral (n, 0) zigzag SWCNTs was considered in our simulations. We selected (7, 0), (13, 0), (19, 0) and (25, 0) zigzag SWCNTs composed of 560, 1040, 1520 and 2000 atoms for the model calculations. The lengths for these tubes were all about 85.20 Å and the diameter ranged from 0.4 nm to 2.0 nm. The simulated diameter corresponded to the actual diameter of nanotubes synthesized in the experiment [28]. As shown in Fig. 1, the selected incident ion was firstly placed 3 nm above the nanotube surface and had negligible interactions with the target atoms. For each tube, a periodic boundary condition along the tube axis was used and non-

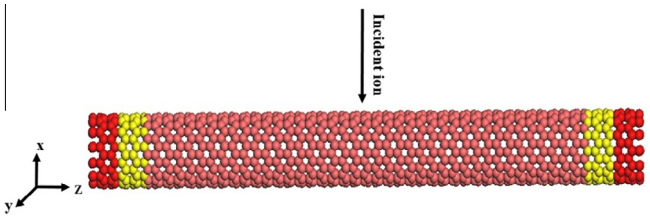

Fig. 1. Side view of the simulation setup used. The incident ion was initially above the surface of SWCNTs. In this model, the yellow atoms close to both ends acted as a thermostat region to maintain a constant temperature; the red atoms were kept fixed during the simulation; and the central region of the thermostat was used to simulate the collision cascades process. (For interpretation of the references to color in this figure legend, the reader is referred to the web version of this article.)

periodic conditions were adopted in the other two dimensions. An initial relaxation phase of 10 ps with a fixed time step of 0.1 fs was applied to equilibrate the system at the NVT ensemble (300 K). A time step of 0.05 fs was used to simulate the ion-SWCNTs interaction during the collision cascades phase. The simulations were carried out for 25 ps. Atoms in the thermostat region were kept at a constant temperature of 300 K through the Nosé-Hoover heat bath, using a coupling constant of 1 ps, so that the excess kinetic energy introduced by the incident ion would be dissipated as that in the experimental situations, and the atoms at both ends of SWCNTs were kept fixed in order to prevent CNTs from being displaced by the transfer of momentum.

The collision process between an energetic ion and SWCNTs was investigated by assigning the energy of incident carbon ion ranging from 25 eV to 1 keV. For each type of SWCNTs, each incident ion energy, each temperature (100 K, 300 K and 700 K) and each ion fluence (2×10^{13}, 6×10^{13}, 1×10^{14} and 2×10^{14}/cm^2), five independent runs were carried out at different sites of SWCNTs and the final results were averaged. The evolution of the system was monitored and then the structural configuration and stability of SWCNTs were analyzed.

3. Results and discussion

In our simulation, we identified the types and abundance of defects which appeared in SWCNTs surface under ion radiation with energies ranging from 25 eV to 1 keV in different models, including a single vacancy, divacancy, adatom, and non-hexagonal rings. To describe the irradiation effects of an incident ion to SWCNTs, we calculated two kinds of defect production quantitatively: the coordination defect number (CDN) and sputtering yield (Y). The CDN is defined as the number of target atoms that have other than three nearest neighbors or bonds, and the Y is defined as the number of target atoms that are sputtered from the SWCNTs surface per incident ion. These two kinds of defect production, to some extent, could reflect the structural configuration and stability of SWCNTs.

3.1. Influence of different incident sites on SWCNTs

The initial positions of an incident ions are randomly distributed on the wall of SWCNTs in actual experiment. However, in our simulation we discover that the defect production of different impinging positions has remarkable differences, therefore it may introduce significant statistical errors. In order to clarify the radiation damage mechanism of SWCNTs at different ion incident sites, we classify the impinging sites of SWCNTs into three specific types in our study, as shown in Fig. 2. The first type is the C atom (Site 1), where an incident ion vertically impacts the carbon atom

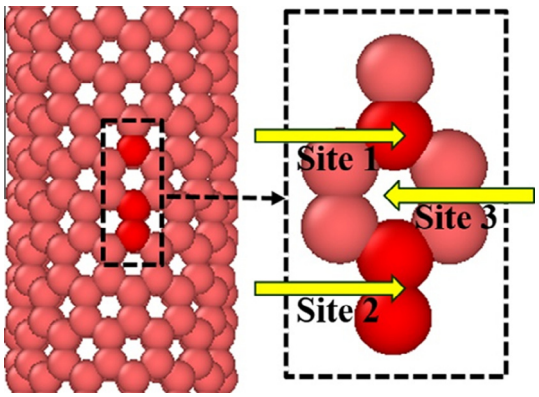

Fig. 2. The sites of SWCNTs are categorized into three types: C atom (Site 1), C–C bond (Site 2), and C-hexagon center (Site 3). Yellow arrows in the magnified image denote the positions of an incident ion. (For interpretation of the references to color in this figure legend, the reader is referred to the web version of this article.)

of SWCNTs. The second type is the C–C bond center (Site 2), where an incident ion vertically impacts the C–C bond center of SWCNTs. The third type is the C-hexagon center (Site 3), where an incident ion vertically impacts on the open structure center of carbon network.

The dependences of CDN and Y of three different sites on incident ion energy were calculated under a single carbon ion irradiation. As shown in Figs. 3 and 4, the CDN and Y reach the maximum values at Site 1, and the CDN and Y of Site 2 and Site 3 are lower than those at Site 1. It should be noted that the error bars of all figures are plotted by using standard deviation. The influence of Site 3 may be ignored as the diameter of SWCNTs increases. To kick out an atom from the lattice, a displacement threshold energy (T_d) must be transferred to the atom. For most types of incident ions, the minimum kinetic energy (E_{min}) of the ion to displace a carbon atom should be substantially larger than T_d required according to classical binary collision theory [7]:

$$E_{min} = T_d(m_c + M)^2/(4m_cM) \quad (1)$$

where m_c and M are the mass of the carbon atom and the ion respectively. This would be a lower bound on the energy, as a part of the energy is always transferred to the atoms neighboring the recoil atom. The energy transferred to the target atom reaches the maximum value for the direct impact at Site 1. Therefore, the maximal damage of SWCNTs occurs at Site 1. Furthermore, an incident ion may enter the lattice at Site 3 and leave from the open structure of SWCNTs on the other side because of the perfect symmetrical structure of carbon nanotubes, and another situation was that some secondary knock-on atoms became adatoms on the inner and outer wall of SWCNTs, thus partly decreasing the CDN and Y at Site 3.

For each model, the CDN and Y of three different sites increase to the maximum value with the increase in incident ion energy, and slightly decrease but keep stable within the majority of the energy range. The initial increases of the CDN and Y with ion energy can be easily interpreted as follows: the low-energy ion simply cannot displace target atoms and the decrease in defect production at the high energies is related to the decrease in the collision cross section for defect production [29]. Moreover, the

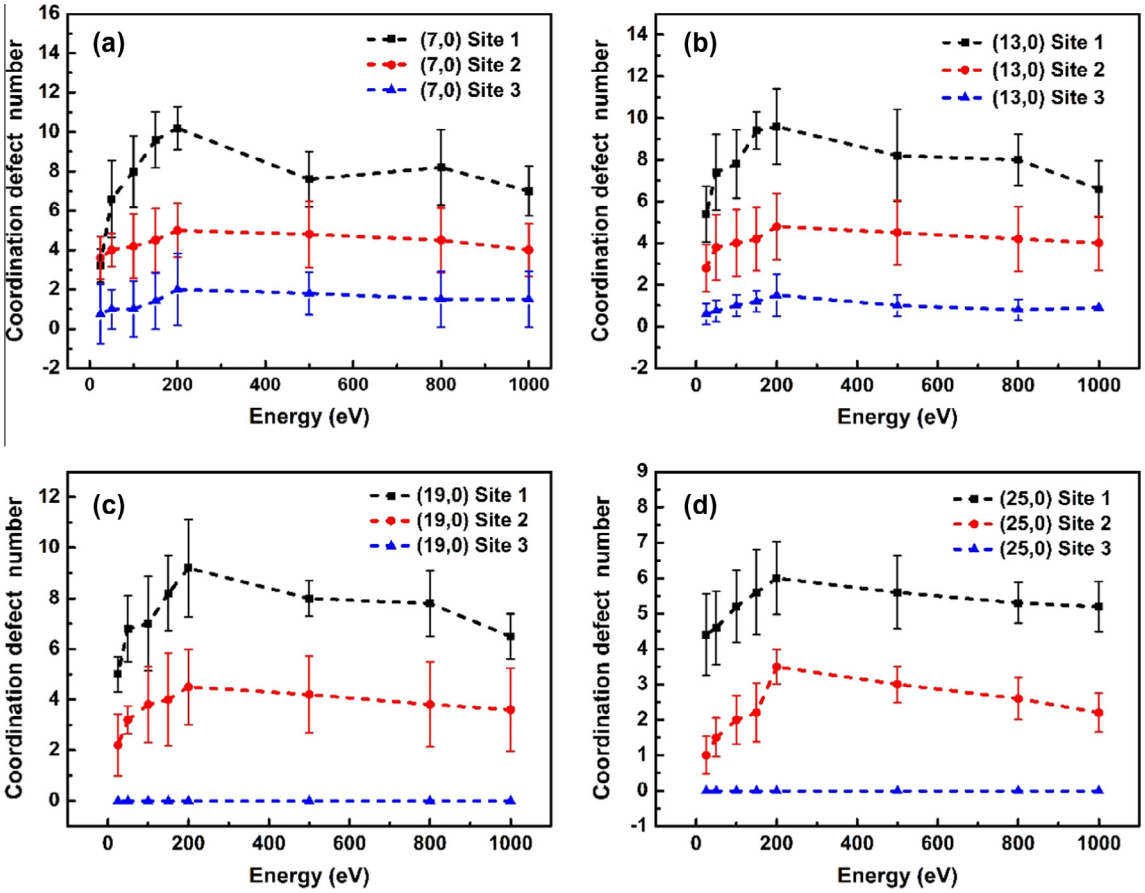

Fig. 3. The coordination defect number (CDN) of Site 1, Site 2, and Site 3 of (a) (7, 0), (b) (13, 0), (c) (19, 0), and (d) (25, 0) zigzag SWCNTs under C ion irradiation with incident energy ranging from 25 eV to 1 keV at room temperature. (Note that the error bars are plotted by using standard deviation, similarly hereinafter.)

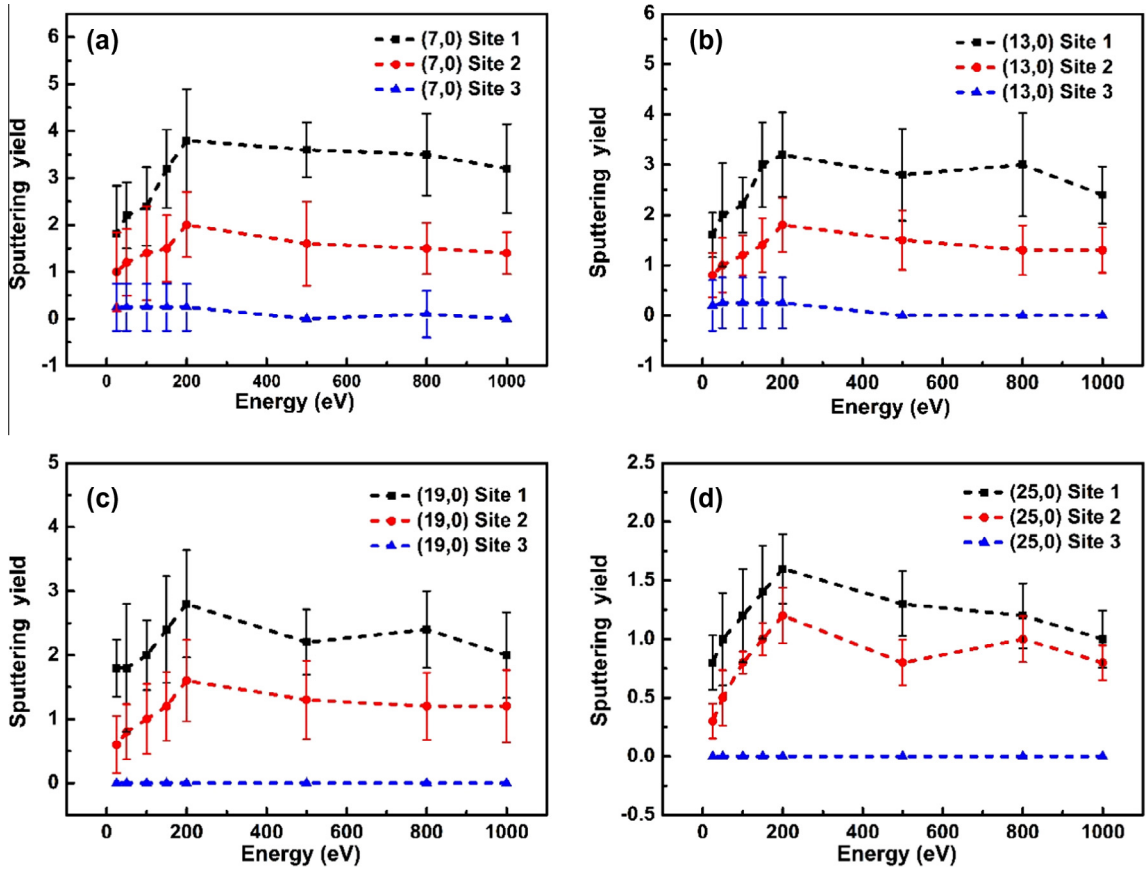

Fig. 4. The sputtering yield (Y) of Site 1, Site 2, and Site 3 of (a) (7, 0), (b) (13, 0), (c) (19, 0), and (d) (25, 0) zigzag SWCNTs under C ion irradiation with incident energy ranging from 25 eV to 1 keV at room temperature.

impacts give rise to morphological changes on the surface of SWCNTs at high energies, including the formation of non-hexagonal ring defects through removing one or two atoms from the target. The obtained structures remain sp^2 hybridized and make the dangling bond of carbon atoms saturated, thus reducing the defect production to some degree.

As illustrated in Figs. 3 and 4, the CDN and Y decrease with the increase in the tube diameter for four tubes. It is well known that the carbon atom of a smaller SWCNTs is easily kicked out because the strain of carbon network is higher and the cohesive energy is smaller, and thus the T_d of carbon atoms in a thinner SWCNT will be smaller correspondingly [30]. Therefore, compared with (13, 0), (19, 0) and (25, 0) CNTs, the damage to thinner (7, 0) CNTs show the extremely severe damage. Moreover, as shown in Fig. 5, the structure of (7, 0) CNTs is largely amorphous within 2 ps under a 200 eV carbon ion bombardment, such as radial shrinkage and bending, whereas (19, 0) and (25, 0) CNTs can maintain its structure stability better. According to the discussion above, the stability of the thicker SWCNTs would be better than the thinner SWCNTs under ion irradiation.

3.2. Influence of temperature on SWCNTs

Temperature affects the evolution of irradiation-induced defects in materials as well as the radiation damage of SWCNTs. Previous experiments on ion irradiation of SWCNTs and its bundles indicated that radiation-induced damage in nanotubes could be readily annealed at the temperature above 300 °C [31].

According to the discussion in Subsection 3.1, the defect production induced by irradiation reaches the maximum value when

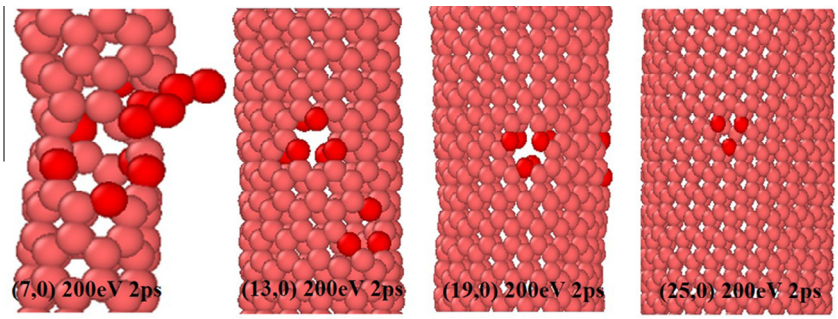

Fig. 5. The structures of four SWCNTs under C incidence within 2 ps at room temperature for 200 eV case.

an incident ion vertically impacts on C atom (Site 1) of SWCNTs. Therefore, the influence of temperature (100 K and 700 K) on SWCNTs is studied under carbon ion incidence at Site 1. As illustrated in Fig. 6, the coordination defect number of the four tubes decrease with temperature rise, and it is clear that the larger the diameter of SWCNTs is, the smaller the coordination defect number is. The same situation occurs at the sputtering yield as well. Furthermore, the result is still consistent with the above conclusion in Subsection 3.1.

The mechanisms of defect annealing at the higher temperature could be explained as follows: one mechanism is vacancy healing through dangling bond saturation and by forming non-hexagonal rings or SW defect [7]. As shown in Fig. 7, the same position of (13, 0) CNTs transforms the divacancy in the carbon network to non-hexagonal rings under a 800 eV carbon ion bombardment over 2 ps at 300 K and 700 K. Furthermore, the local diameter reduction will be caused by this structure transformation. The other mechanism is that the migration rate of carbon interstitials increases at the higher temperature and then interstitials may combine with certain vacancies, which reduces the coordination defect number significantly. In addition, it should be noted that irradiation-induced defects may also heal at lower temperature because of a non-thermal graphene network restructuring mechanism [19], but this process is simply not observed in our study due to the short simulation time scale. Therefore, SWCNTs have the unique ability to heal the radiation-induced damage at the higher temperature, which is beneficial to the development of SWCNTs-based materials.

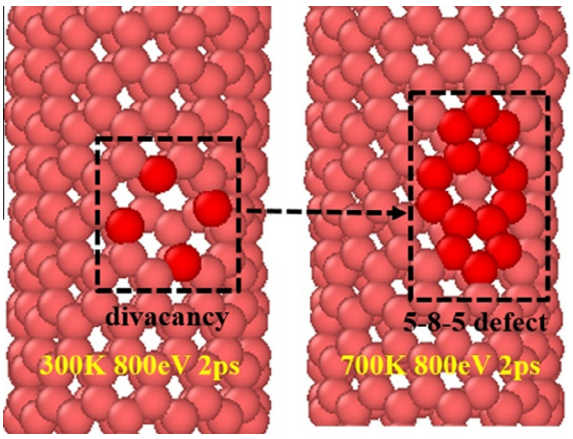

Fig. 7. The same position of (13, 0) SWCNTs transforms the divacancy in the carbon network to non-hexagonal rings (i.e. 5-8-5 defect) under a 800-eV carbon ion bombardment over 2 ps at 300 K and 700 K.

3.3. Influence of irradiation fluence on SWCNTs

Multiple defects generated by ion irradiation showed an important influence on the material performance. In Subsection 3.1, we mainly studied single impinging ion, which actually corresponded to the case of the low ion fluence. The structural response of SWCNTs to ion irradiation had been systematically studied with the increasing irradiation fluence as a function of SWCNTs-diameter distribution [32].

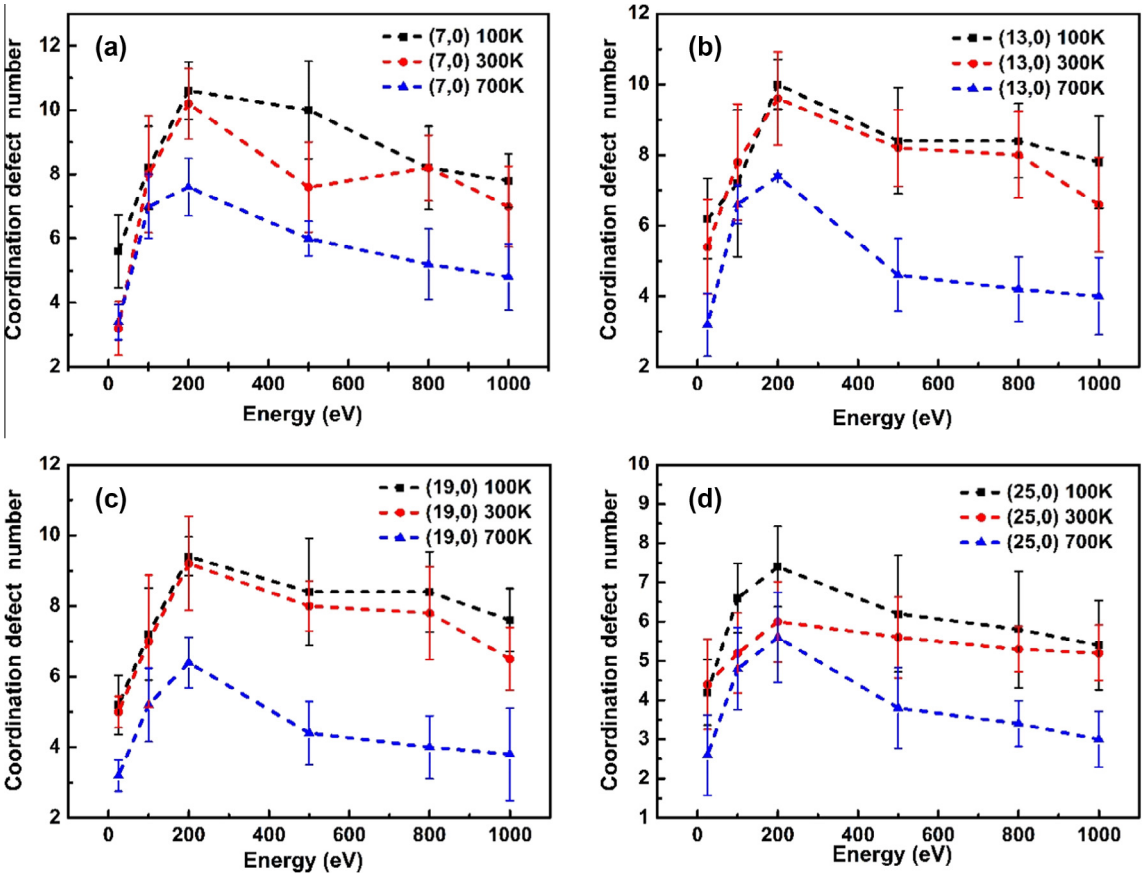

Fig. 6. The coordination defect number of (a) (7, 0), (b) (13, 0), (c) (19, 0), and (d) (25, 0) zigzag SWCNTs under C ion irradiation with incident energy ranging from 25 eV to 1 keV at 100 K, 300 K, and 700 K at Site 1.

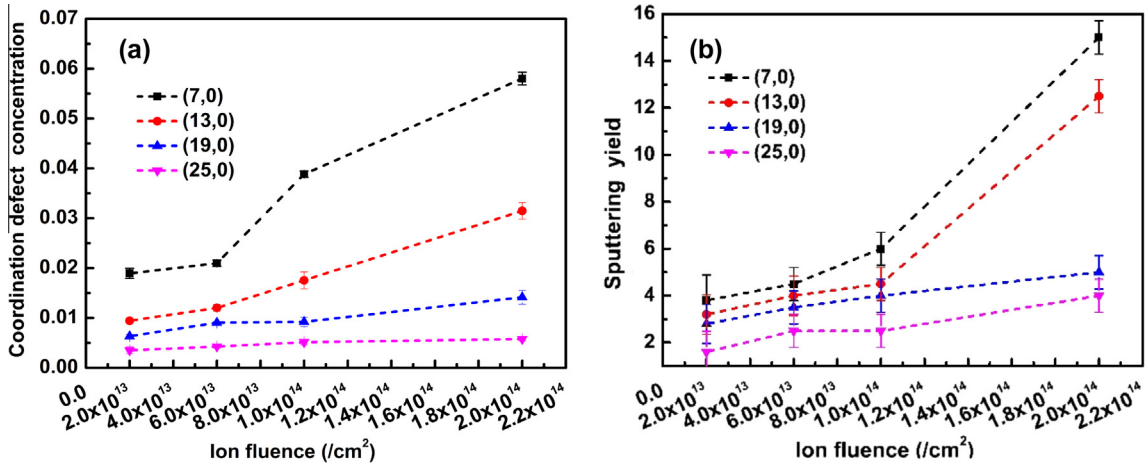

Fig. 8. The (a) coordination defect concentration and (b) sputtering yield of four zigzag SWCNTs under different incident ion fluences at 300 K.

As shown in Figs. 3 and 4, the CDN and Y reach the maximum values under the 200-eV carbon ion bombardment. We investigated the influence of four SWCNTs exposed to different ion fluences (2×10^{13}, 6×10^{13}, 1×10^{14}, and 2×10^{14}/cm^2) under 200 eV, which corresponded to the results by N.P. O'Brien [15]. Importantly, we should guarantee the identical ion fluence of four SWCNTs per unit area because of their different diameters. For the four carbon nanotubes, the same bombardment area (5.79 Å × 83.86 Å) was chosen to simulate each radiation event under different ion fluences. We defined the coordination defect concentration as the coordination defect number divided by the total atoms number of SWCNTs to describe the defect production mechanism in the high-fluence circumstance. As illustrated in Fig. 8, the coordination defect concentration and sputtering yield of four SWCNTs uniformly increase with the carbon ion fluence rise, and the variation of the thinner tube has a sharp rise compared with a large diameter tube. The damage of SWCNTs under the high ion fluence would be serious. The results were consistent with previous results reported by Saraiva [33].

4. Conclusions

In order to better understand the radiation damage and microstructure evolution at a nanoscale time, we investigated carbon ion irradiation of single-walled carbon nanotubes (SWCNTs) in detail with state-of-the-art reactive molecular dynamics simulations. We classified the different sites of SWCNTs into three categories for the first time. The radiation damage of SWCNTs under incident carbon ion with energy ranging from 25 eV to 1 keV at room temperature shows significant differences at different sites and the difference in the damage level reaches several orders in our simulations (Site 1 > Site 2 > Site 3). That is to say, the damage level to SWCNTs will be the worst when the incident ion directly impacts on the carbon atom. Both the coordination defect number and sputtering yield increase to the maximum value with the increase in incident ion energy, and slightly reduce but keep stable within the majority of the energy range. It should be pointed out that the defect level becomes excessive if the incident ion fluence is set too high and amorphization occurs at the highest level of fluence. The above phenomena are also studied at 100 K and 700 K and the defect production decreases distinctly with the temperature rise because irradiation-induced defects would anneal and recombine through making the dangling bond saturated and carbon network reconstructed at the higher temperature. SWCNTs have the surprisingly high ability to heal the irradiation-induced damage, which should facilitate the nanotechnology of CNTs-based composites. Generally speaking, we find that the stability of SWCNTs with a large-diameter would be better than a slim one under the same irradiation conditions. The fundamental information of ion-irradiation-induced phenomena in SWCNTs could provide essential guidelines for developing the CNTs-based devices in extreme radiation environments.

These results may be conductive to understand the defect production mechanism and defect microstructure evolution of zigzag carbon nanotubes under ion irradiation. However, other factors such as chirality parameters of SWCNTs, different types and impact angles of incident ions are still significant, therefore further studies are to be carried out in our work.

Acknowledgements

This work was supported by the Priority Academic Program Development of Jiangsu Higher Education Institutions, the Specialized Research Fund for the Doctoral Program of Higher Education of China (SRFDP) (Grant No. 20133218110023), and the Funding of Jiangsu Innovation Program for Graduate Education (Grant No. KYLX15_0306).

Appendix A. Supplementary data

Supplementary data associated with this article can be found, in the online version, at http://dx.doi.org/10.1016/j.nimb.2016.04.043.

References

[1] A.D. Franklin, S.O. Koswatta, D.B. Farmer, et al., Carbon nanotube complementary wrap – Gate transistors, Nano Lett. 13 (2013) 2490–2495.
[2] J.M. Schnorr, T.M. Swager, Emerging applications of carbon nanotubes, Chem. Mater. 23 (2011) 646–657.
[3] S. Dong, J. Zhou, D. Hui, Y. Wang, S. Zhang, Size dependent strengthening mechanisms in carbon nanotube reinforced metal matrix composites, Compos. Part A: Appl. Sci. Manuf. 68 (2015) 356–364.
[4] L. Ge, S. Sethi, L. Ci, P.M. Ajayan, Carbon nanotube-based synthetic gecko tapes, Proc. Natl. Acad. Sci. U.S.A. 104 (2007) 10792–10795.
[5] B.D. Weaver, B.J. Landi, R.P. Raffaelle, High radiation tolerance of carbon nanotube matrices for space power applications, in: 2nd International Energy Conversion Engineering Conference, 2004.
[6] C.D. Denton, J.C. Moreno-Marin, S. Heredia-Avalos, Energy distribution of the particles obtained after irradiation of carbon nanotubes with carbon projectiles, Nucl. Instr. Meth. Phys. Res. B 352 (2015) 221–224.
[7] A.V. Krasheninnikov, K. Nordlund, Ion and electron irradiation-induced effects in nanostructured materials, J. Appl. Phys. 107 (2010) 071301.

[8] A. Olejniczak, V.A. Skuratov, Effect of swift heavy ion irradiation on single- and multiwalled carbon nanotubes, Nucl. Instr. Meth. Phys. Res. B 326 (2014) 33–36.
[9] H. Huang, X. Tang, F. Chen, Y. Yang, J. Liu, H. Li, D. Chen, Radiation damage resistance and interface stability of copper-graphene nanolayered composite, J. Nucl. Mater. 460 (2015) 16–22.
[10] J.A.V. Pomoell, A.V. Krasheninnikov, K. Nordlund, J. Keinonen, Ion ranges and irradiation-induced defects in multiwalled carbon nanotubes, J. Appl. Phys. 96 (2004) 2864.
[11] A.V. Krasheninnikov, K. Nordlund, Irradiation effects in carbon nanotubes, Nucl. Instr. Meth. Phys. Res. B 216 (2004) 355–366.
[12] M.S. Raghuveer, P.G. Ganesan, J. D'Arcy-Gall, G. Ramanath, Nanomachining carbon nanotubes with ion beams, Appl. Phys. Lett. 84 (2004) 4484.
[13] M. Khazaei, A. Farajian, G. Jeong, et al., Dynamical criteria for Cs ion insertion and adsorption at cap and stem of carbon nanotubes: ab initio study and comparison with experiment, J. Phys. Chem. B 108 (2004) 15529–15535.
[14] T. Kato, E.C. Neyts, Y. Abiko, et al., Kinetics of energy selective Cs encapsulation in single-walled carbon nanotubes for damage-free and position-selective doping, J. Phys. Chem. C 119 (2015) 11903–11908.
[15] N.P. O'Brien, M.A. McCarthy, W.A. Curtin, Improved inter-tube coupling in CNT bundles through carbon ion irradiation, Carbon 51 (2013) 173–184.
[16] E. Salonen, A.V. Krasheninnikov, K. Nordlund, Ion-irradiation-induced defects in bundles of carbon nanotubes, Nucl. Instr. Meth. Phys. Res. B 193 (2002) 603–608.
[17] S.K. Pregler, B.W. Jeong, S.B. Sinnott, Ar beam modification of nanotube based composites using molecular dynamics simulations, Compos. Sci. Technol. 68 (2008) 2048–2055.
[18] Z. Xu, W. Zhang, Z. Zhu, C. Ren, Effects of tube diameter and chirality on the stability of single-walled carbon nanotubes under ion irradiation, J. Appl. Phys. 106 (2009) 043501.
[19] E.C. Neyts, K. Ostrikov, Z.J. Han, et al., Defect healing and enhanced nucleation of carbon nanotubes by low-energy ion bombardment, Phys. Rev. Lett. 110 (2013) 065501.
[20] E.C. Neyts, A. Bogaerts, Ion irradiation for improved graphene network formation in carbon nanotube growth, Carbon 77 (2014) 790–795.
[21] R.K. Baik, C.R. Abernathy, S.J. Pearton, et al., Proton irradiation of ZnO schottky diodes, J. Electron. Mater. 34 (2005) 395–398.
[22] S. Plimpton, Fast parallel algorithms for short-range molecular dynamics, J. Comput. Phys. 117 (1995) 1–19.
[23] S.J. Stuart, A.B. Tutein, J.A. Harrison, A reactive potential for hydrocarbons with intermolecular interactions, J. Chem. Phys. 112 (2000) 6472.
[24] J. Tersoff, New empirical approach for the structure and energy of covalent systems, Phys. Rev. B 39 (1989) 5566–5568.
[25] J.F. Ziegler, J.P. Biersack, U. Littmark, The Stopping and Ranges of Ions in Matter, Pergamon, New York, 1985.
[26] S. Zhao, J. Xue, Y. Wang, S. Yan, Chemical bonding assisted damage production in single-walled carbon nanotubes induced by low-energy ions, Appl. Phys. A Mater. 108 (2012) 313–320.
[27] K. Nordlund, J. Keinonen, Formation of ion irradiation induced small-scale defects on graphite surfaces, Phys. Rev. B 77 (1996) 2.
[28] G. Gao, T. Cagin, W.A. Goddard, Energetic, structure, mechanical and vibrational properties of single-walled carbon nanotubes, Nanotechnology 9 (1998) 184–191.
[29] O. Lehtinen, J. Kotakoski, A.V. Krasheninnikov, et al., Effects of ion bombardment on a two-dimensional target: atomistic simulations of graphene irradiation, Phys. Rev. B 81 (2010) 153401.
[30] A.V. Krasheninnikov, F. Banhart, J.X. Li, A.S. Foster, Stability of carbon nanotubes under electron irradiation: role of tube diameter and chirality, Phys. Rev. B 72 (2005) 125428.
[31] F. Banhart, Irradiation effects in carbon nanostructures, Rep. Prog. Phys. 62 (1999) 1181.
[32] J.E. Rossi, C.D. Cress, A. Merrill, K.J. Soule, N.D. Cox, B.J. Landi, Intrinsic diameter dependent degradation of single-walled carbon nanotubes from ion irradiation, Carbon 81 (2014) 488–496.
[33] G.D. Saraiva, A.G. Souza Filho, Braunstein, et al., Resonance raman spectroscopy in Si and C ion-implanted double-wall carbon nanotubes, Phys. Rev. B 80 (2009) 155452.